Stolt prestack residual migration for converted waves

Daniel Rosales, Biondo Biondi and Paul Sava, Geophysics Department, Stanford University*

SUMMARY

PS velocity analysis is an important aspect of converted wave seismic imaging. To obtain one consistent image, it is necessary to correctly derive both the *P*-wave and the *S*-wave velocity models. Stolt prestack residual migration is a useful technique for velocity analysis and image update. This paper extends Stolt prestack residual migration to handle two different velocity fields. The new operator that we introduce is promising for *PS* velocity analysis. We present a theoretical discussion of our new operator and discuss its ability to focus *PS* images. Finally, we present prestack residual migration results on a synthetic and a real dataset.

INTRODUCTION

Residual migration is an useful tool to improve the quality of the image and to perform migration velocity analysis (Sava, 2000a,b). It is possible to update the image with low cost because it is not necessary to re-run the entire migration process. Al-Yahya and Fowler (1986; 1989) discuss a residual migration operator in the prestack domain, and show that it can be posed as a function of a non-dimensional parameter that is the ratio of the correct velocity and the reference velocity used for the initial migration. Residual migration is more accurate than residual moveout after migration because the events move horizontally as well as vertically. It is crucial to have an operator able to handle two different velocity fields to perform prestack residual migration for converted waves. Stolt (1996) defines a prestack residual migration operator in the (ω,k) domain. Sava (2000a) reformulates Stolt prestack residual migration operator as a function of a non-dimensional parameter that is the ratio of the reference and correct velocities. We present a Stolt prestack residual migration operator able to handle two different velocity fields, therefore it is useful for converted waves imaging and velocity analysis.

Stolt residual migration extends to converted waves in two different ways: an exact derivation and an approximate one. This leads to three methods for Stolt prestack residual migration for converted waves. The methods vary on the number of independent parameters for image update. The exact method calculates an appropriate transformation kernel that is able to handle both velocity fields. The exact method uses three independent parameters for image update. The approximate methods uses only two independent parameters for image update.

We discuss the advantages and disadvantages of the three methods. We also show synthetic examples. Real data results will be presented in the conference.

THEORY

Stolt (1996) first introduces prestack residual migration. Sava (2000a) reformulates Stolt residual migration in order to handle prestack depth images. We extend Sava's (2000a) formulation in order to handle two different velocity fields. We present this extension for converted waves data, where the *P* to *S* conversion occurs at the reflector.

Stolt prestack residual migration operates in the Fourier domain. Considering the representation of the input data in shot-geophone coordinates, the mapping from the data space to the model space takes the form

$$k_z = \frac{1}{2}\left(\sqrt{\frac{\omega^2}{v_p^2} - k_s^2} + \sqrt{\frac{\omega^2}{v_s^2} - k_g^2}\right), \tag{1}$$

where k_s, k_g, v_p, and v_s stand for, respectively, the source and geophone wavenumbers, and the *P* and *S* velocities.

With Stolt prestack residual migration for converted waves, we attempt to simultaneously correct the effects of migrating with two inaccurate velocity fields. Assuming that v_{0p} and v_{0s} are the initial migration velocities and v_{mp} and v_{ms} are the correct velocities, we can then write

$$\begin{cases} k_{z_0} = \frac{1}{2}\left(\sqrt{\frac{\omega^2}{v_{0p}^2} - k_s^2} + \sqrt{\frac{\omega^2}{v_{0s}^2} - k_g^2}\right) \\ k_{z_m} = \frac{1}{2}\left(\sqrt{\frac{\omega^2}{v_{mp}^2} - k_s^2} + \sqrt{\frac{\omega^2}{v_{ms}^2} - k_g^2}\right). \end{cases} \tag{2}$$

This system of equations is the basis for Stolt prestack residual migration. We can observe that residual migration depends on four parameters v_{0p}, v_{0s}, v_{mp} and v_{ms}.

We present three methods for performing Stolt prestack residual migration for converted waves. The methods vary on both the number of independent parameters for residual migration and the definition of the kernel that transforms the image with the wrong velocity model to a new, more accurate, image.

The first method is the exact method. Solving for ω^2 in the first equation of (2) and substituting into the second equation of (2), we obtain the expression for Stolt prestack residual migration for converted waves [equations (3) or (4)]

$$k_{z_m} = \tfrac{1}{2}\sqrt{\rho_p^2\kappa_0^2 - k_s^2} + \tfrac{1}{2}\sqrt{\rho_s^2\gamma_0{}^2\kappa_0^2 - k_g^2}, \tag{3}$$

or

$$k_{z_m} = \tfrac{1}{2}\sqrt{\rho_p^2\kappa_0^2 - k_s^2} + \tfrac{1}{2}\sqrt{\rho_p^2\gamma_m{}^2\kappa_0^2 - k_g^2}, \tag{4}$$

where $\rho_p = \frac{v_{0p}}{v_{mp}}$, $\rho_s = \frac{v_{0s}}{v_{ms}}$, and $\gamma = \frac{v_p}{v_s}$.

κ_0^2 is the transformation kernel that is defined as

$$\kappa_0^2 = \frac{A - B}{(\gamma_0{}^2 - 1)^2}, \tag{5}$$

where

$$\begin{aligned} A &= 4(\gamma_0{}^2 + 1)k_{z_0}{}^2 + (\gamma_0{}^2 - 1)(k_g{}^2 - k_s{}^2), \\ B &= 4k_{z_0}\sqrt{(1-\gamma_0{}^2)(\gamma_0{}^2 k_s{}^2 - k_g{}^2) + 4\gamma_0{}^2 k_{z_0}{}^2}. \end{aligned}$$

Equations (3) and (4) are two equivalent ways of expressing the exact derivation of Stolt prestack residual migration. We can observe that the four parameters in equation (2) reduce to three in

equations (3) and (4) (ρ_p, ρ_s and γ). This is important, because a three parameters search for updating converted waves images is simpler than a four parameters search. However, it would be useful to further reduce the number of parameters.

The effort to further reduce the number of parameters leads to the second method. Assuming that the v_p/v_s ratio is the same before and after the residual migration process, it is possible to simplify equations (3) and (4) into a two parameter equation:

$$k_{z_m} = \tfrac{1}{2}\sqrt{\rho_p^2\overline{\kappa}_0^2 - k_s^2} + \tfrac{1}{2}\sqrt{\rho_p^2\gamma^2\overline{\kappa}_0^2 - k_g^2}, \tag{6}$$

where the transformation kernel ($\overline{\kappa}_0^2$) takes the form

$$\overline{\kappa}_0^2 = \frac{A-B}{(\gamma^2-1)^2}, \tag{7}$$

and

$$\begin{aligned} A &= 4(\gamma^2+1){k_{z_0}}^2 + (\gamma^2-1)({k_g}^2 - {k_s}^2), \\ B &= 4k_{z_0}\sqrt{(1-\gamma^2)(\gamma^2{k_s}^2 - {k_g}^2) + 4\gamma^2{k_{z_0}}^2}. \end{aligned}$$

The third method also involves a two parameters search. If we just specify two different ratios in both square roots of Sava's (2000a) formulation we have

$$k_{z_m} = \tfrac{1}{2}\sqrt{\rho_p^2\overline{\overline{\kappa}}_0^2 - k_s^2} + \tfrac{1}{2}\sqrt{\rho_s^2\overline{\overline{\kappa}}_0^2 - k_g^2}, \tag{8}$$

where the transformation kernel ($\overline{\overline{\kappa}}_0^2$) has the same form as the one of *PP* waves:

$$\overline{\overline{\kappa}}_0^2 = \frac{\left[4k_{z_0}^2 + (k_g - k_s)^2\right]\left[4k_{z_0}^2 + (k_g + k_s)^2\right]}{16k_{z_0}^2}. \tag{9}$$

The third method distinguishes from the second one in the definition of the transformation kernel. The transformation kernel for the second method [equation (7)] is an accurate derivation for converted waves. But, the transformation kernel for the third method [equation (9)] is exactly the same as the *PP* case. Therefore, it will not be able to handle the asymmetry of converted waves data properly.

It is important to note that all three equations (3), (6), and (8) reduce to the same expressions in the limit when v_s tends to v_p, or γ tends to 1. All of them reduce to the simple case of prestack residual migration for conventional *PP* data.

NUMERICAL EXAMPLES

Impulse Responses

Figure 1 shows the impulse response for the three methods of the Stolt prestack residual migration operators for converted waves [equations (3), (6) and (8)].

Figure 1a presents the impulse response for the first method, with $\rho_p = 1.2$, $\rho_s = 1.3$ and $\gamma_0 = 2$. Figure 1b presents the impulse response for the second method, with $\rho_p = 1.2$ and $\gamma = 2$. Figure 1c shows the impulse response for the third method with $\rho_p = 1.2$, $\rho_s = 1.3$.

We can observe the differences in the three methods. Method one gives a more accurate and a wider distribution of the energy. While methods two and three have a more limited distribution of the energy.

Between methods two and three the smaller elliptical response of method three is due to the use of a transformation kernel not designed to handle the duality of two different velocity fields.

Residual migration with constant velocity

In order to test the accuracy of our operator we created a synthetic data set assuming a constant velocity model of $v_p = 3000$ m/s and $v_s = 1500$ m/s, and four reflectors having dips of 15°, 0°, −30° and −45°.

We first migrate the data using shot-profile migration with the correct *P* velocity model and a +15% perturbation in the *S* velocity model. We extract angle-domain common-image gathers for converted waves (Rosales and Rickett, 2001; Rickett and Sava, 2001). We then apply Stolt prestack residual migration, using the three previous methods.

Figure 2 shows angle domain common image gathers (de Bruin et al., 1991; Prucha et al., 1999) all taken at the same surface location. The top, center and bottom panels exhibit the migration with the wrong velocity model, the residual migration result with method number one and the migration result with the correct velocity model, respectively. The major difference is in the third event, which corresponds to the −30° layer. The top panel shows a moveout pointing downward. Residual migration makes the moveout comparable to the moveout after migration with the correct velocity model.

Figure 3 shows the final stack section, after reversing the polarities in the angle domain (Rosales and Rickett, 2001), for the residual migration and the migration with the correct velocity model. It is possible to observe that the two images are highly correlated. It is also possible to observe artifacts, in the residual migration result, due to the Fourier transformation. Migration with the wrong velocity model partially destroys some events. Therefore, the lost energy in the migration process can not be recovered in the residual migration process.

Residual migration with depth variant velocity

Stolt prestack residual migration for converted waves assumes constant velocity. Sava (2000b) evaluates the use of Stolt prestack residual migration in a depth variant velocity media. Method one, the exact method, formulates residual migration with three parameters. Because the three parameters are only velocity ratios, the method is not restricted to constant velocity media. We present a synthetic example that involves depth variable velocities.

The second synthetic model uses the same reflector geometry as the previous one but it now uses a realistic depth velocity model of $v_{0p} = 1700$ m/s and a gradient of 0.15 s^{-1} and $v_{0s} = 300$ m/s and a gradient of 0.35 s^{-1},

We perform the initial shot profile migration with a 15% positive perturbation in the *S*-velocity model. Figure (4) presents three angle domain common image gathers. From top to bottom: migration result with the wrong velocity model, residual migration and migration result with the correct velocity model. The velocity model is depth variant, therefore a single value for the three parameters does not correct the entire image. It is thus necessary to correctly select the right combination of parameters for different depth steps that will improve the entire image.

The results in Figure (4) are for a specific selection of $\rho_p = 1$, $\rho_s = 1.15$ and $\gamma_0 = 1.92$, these values are the RMS values for a

depth of 800 m. This is the depth for the first event (15° reflector).

Note in Figure (4)a that the first event has a moveout curving downward because of the wrong velocity model. The same event is flat after residual migration with the above values [Figure (4)b]. The residual migration result compares favorably with the migration result with the correct velocity model.

Observe that the second event is flat after residual migration. However, its depth position is wrong. The use of parameters that work only for an specific depth explains this result.

CONCLUSIONS

We introduced the extension of Stolt prestack residual migration for converted waves. Our new operator involves the selection of three parameters in order to update the image.

To help in memory and disk space necessary for the implementation of our operator, we derived approximations that reduce the number of free parameters from three to two. The most appropriate way of reducing the number of parameters is by freezing one of them.

In constant velocity, we proved that we can recover the image obtained with an initial migration that uses an inaccurate *P* and/or *S* velocity models. Therefore, we can update a migration with constant *P* and/or *S* velocity models using our new operator. We can also update an image obtained with a depth variant velocity. The refocusing with residual migration depends on an appropriate parameter picking.

Having an operator to update converted waves images allow us to extend our ability to handle multiple mode data. Therefore, it will lead to more accurate methods for performing velocity analysis for converted waves.

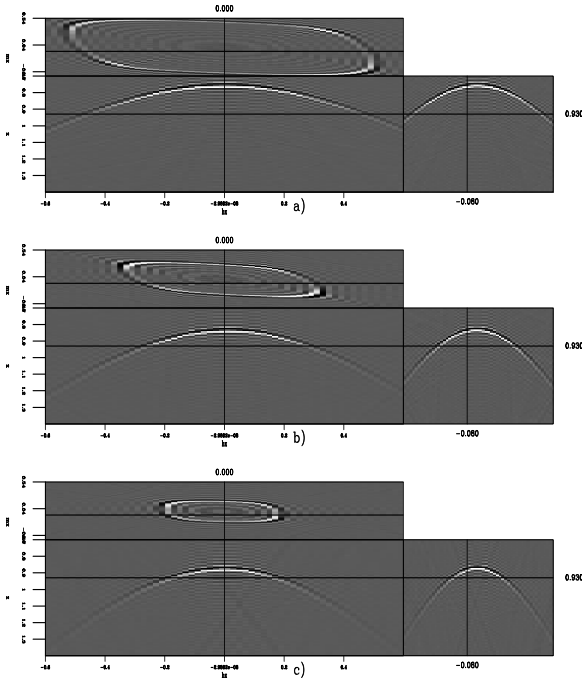

Figure 1: Impulse response for the residual prestack migration operators. From top to bottom, a) equation (3) for $\rho_p = 1.2$, $\rho_s = 1.2$, $\gamma_0 = 2$; b) equation (6) for $\rho_p = 1.3$, $\gamma = 2$; c) equation (8) for $\rho_p = 1.3$, $\rho_s = 1.2$.

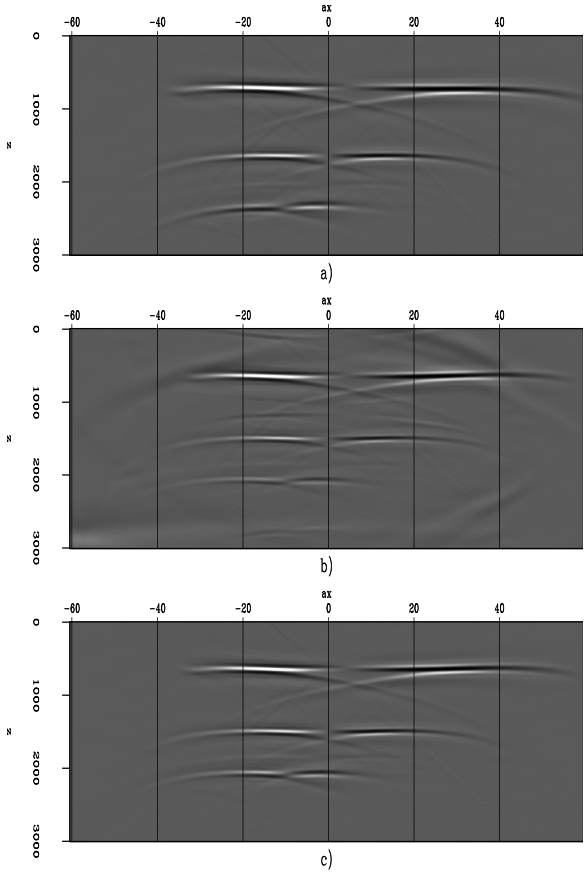

Figure 2: Angle domain common image gathers from top to bottom: a) migration with 15% error in the *S*-velocity; b) residual migration with method one; c) migration with the correct velocity. Observe the difference in the moveout of the bottom event. Panel a) shows a moveout pointing downward for the bottom event. Panel b) shows that the same events is flat after residual migration. The residual migration result totally resembles the migration with the correct velocity model [panel c)].

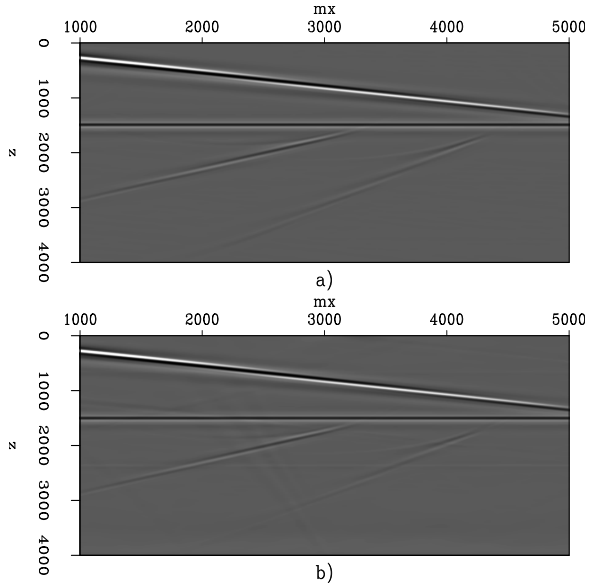

Figure 3: Final stack, after reversing the polarities in the angle domain (Rosales and Rickett, 2001), after: a) residual migration with method one and b) migration with the correct velocity. Note that both results are highle correlated. Panel a) presents some artifacts due to the Fourier domain transformation needed by residual migration.

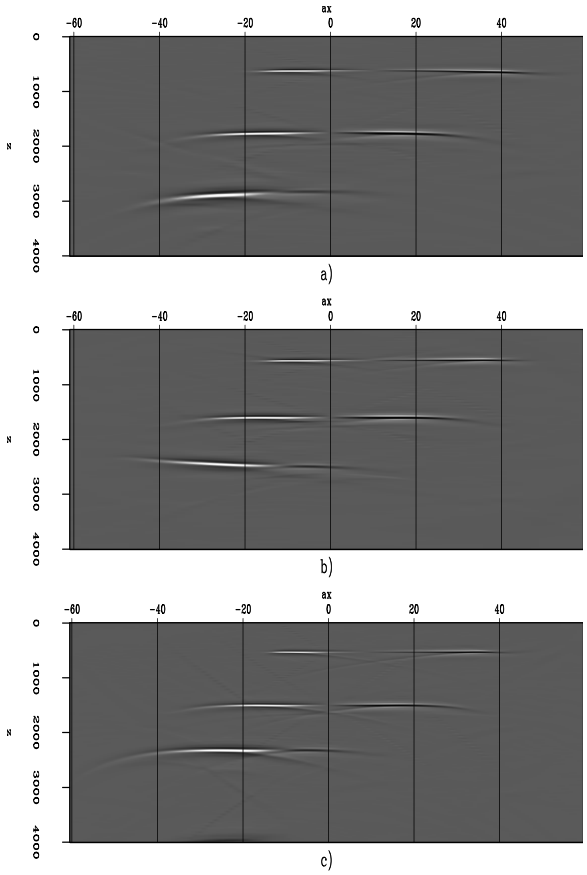

Figure 4: Angle domain common image gathers from top to bottom: a) migration with 15% error in the *S*-velocity model; b) residual migration with method one with $\rho_p = 1$, $\rho_s = 1.15$ and $\gamma_0 = 1.92$; c) migration with the correct velocity model. Panel a) shows the top event with a moveout pointing downward. The others two events also manifest the same overmigration effect. Panel b) exhibits the top event totally flat and in the correct depth position. The center event is also flat but it is in the wrong depth position. The bottom event is now undermigrated. Only one set of parameters, for a specific depth, was used for all the residual migration. Therefore, residual migration will only correct for that specific depth. A parameter picking is necessarilly for a more appropriate result in the entire image.

REFERENCES

Al-Yahya, K., and Fowler, P., 1986, Prestack residual migration: SEP–**50**, 219–230.

Al-Yahya, K. M., 1989, Velocity analysis by iterative profile migration: Geophysics, **54**, no. 06, 718–729.

de Bruin, C. G. M., Wapenaar, C. P. A., and Berkhout, A. J., 1991, Angle-dependent reflectivity by means of prestack migration: Geophysics, **55**, no. 9, 1223–1234.

Prucha, M., Biondi, B., and Symes, W., 1999, Angle-domain common image gathers by wave-equation migration: 69th Annual Internat. Mtg., Society Of Exploration Geophysicists, Expanded Abstracts, 824–827.

Rickett, J., and Sava, P., 2001, Offset and angle domain common image gathers for shot-profile migration: 71st Annual Internat. Mtg., Society Of Exploration Geophysicists, Expanded Abstracts.

Rosales, D., and Rickett, J., 2001, PS-wave polarity reversal in angle domain common-image gathers: 71st Annual Internat. Mtg., Society Of Exploration Geophysicists, Expanded Abstracts, 1843–1845.

Sava, P., 2000a, Prestack stolt residual migration for migration velocity analysis: 70th Annual Internat. Mtg., Society Of Exploration Geophysicists, Expanded Abstracts, 992–995.

Sava, P., 2000b, Variable-velocity prestack Stolt residual migration with application to a North Sea dataset: SEP–**103**, 147–157.

Stolt, R. H., 1996, Short note - a prestack residual time migration operator: Geophysics, **61**, no. 2, 605–607.